Toxicology in Vitro 102 (2025) 105958

Contents lists available at ScienceDirect

Toxicology in Vitro

journal homepage: www.elsevier.com/locate/toxinvit

Curcumin-loaded emulsome nanoparticles induces apoptosis through p53 signaling pathway in pancreatic cancer cell line PANC-1

Zuleyha Demirci [a,b], Zeynep Islek [c], Halime Ilhan Siginc [c], Fikrettin Sahin [c], Mehmet H. Ucisik [c,d,e,**], Zeynep Busra Bolat [a,f,*]

[a] Experimental Medicine Research and Application Center, Validebag Research Park, University of Health Sciences, 34662 Istanbul, Uskudar, Türkiye
[b] Department of Chemistry, Faculty of Art and Science, Yildiz Technical University, 34220 Istanbul, Türkiye
[c] Department of Genetics and Bioengineering, Faculty of Engineering, Yeditepe University, Kayisdagi Cad., 34755 Atasehir, Istanbul, Türkiye
[d] Department of Biomedical Engineering, School of Engineering and Natural Sciences, Istanbul Medipol University, Ekinciler Cad. 19, 34810 Istanbul, Beykoz, Türkiye
[e] Regenerative and Restorative Medicine Research Center (REMER), Research Institute for Health Sciences and Technologies (SABITA), Istanbul Medipol University, Ekinciler Cad. 19, 34810 Istanbul, Beykoz, Türkiye
[f] Molecular Biology and Genetics Department, Hamidiye Institute of Health Sciences, University of Health Sciences, 34668 Istanbul, Uskudar, Türkiye

ARTICLE INFO

Editor: Martin Leonard

Keywords:
Pancreatic cancer
Curcumin
Curcumin nanoformulation
p53 pathway
Anticancer therapy

ABSTRACT

Pancreatic cancer is a global health problem with a poor prognosis, limited treatment options and low survival rates of patients. Thus, the exploration of novel treatment approaches is crucial. Curcumin shows promise in pancreatic cancer. Curcumin has anticancer properties promoting apoptosis through the p53 pathway. However, adverse effects and low bioavailability are curcumin's main drawbacks and its delivery by nanoparticles could improve its effectiveness as a treatment option. Curcumin-loaded emulsome nanoparticles (CurEm) have shown promise in colorectal, hepatocellular, and prostate cancers. This study aims to evaluate the anticancer potential of CurEm in pancreatic cancer cell line PANC-1. The cytotoxic effects of CurEm on PANC-1 cells show cytotoxicity in dose and time-dependent manner. The selected dose 30 μM CurEm resulted spheroidal morphology in PANC-1 cells and colony forming and scratch assay conducted demonstrated significant growth inhibition and decrease in migration ability, respectively. Cell cycle analysis shows that CurEm induces G2/M arrest in PANC-1 cells. CurEm-treated PANC-1 cells showed a significant increase in p53 and Caspase 3 genes, while a significant decrease in Bcl-2 genes compared to untreated group. Western blot results showed parallel results to qPCR analysis for Bcl-2 protein levels. Interestingly, we saw low p53 protein levels in CurEm-treated PANC-1 cells. These findings shed light on the potential of CurEm as an effective and stable therapeutic approach for pancreatic cancer.

1. Introduction

Pancreatic cancer is an aggressive and malignant type of cancer, which ranks twelfth in incidence and seventh in mortality worldwide. It has a higher incidence in men than in women (Sung et al., 2021). Pancreatic cancer is a devastating disease with poor prognosis. As it is asymptomatic during its development, diagnosis is usually made in the advanced stages of the disease or after metastasis (Gillen et al., 2010). Surgical techniques, radiotherapy, and chemotherapy are the current therapeutic approaches, with low survival rates of patients (Gillen et al., 2010; McGuigan et al., 2018). Clinical applications of chemotherapy are limited due to gained drug resistance to the therapies and adverse side effects on healthy tissues (Huang et al., 2022). New therapeutic approaches have become necessary to enable effective and safe treatment of pancreatic cancer. Medical plants known for their intrinsic anti-inflammatory and anti-cancer activities take particular attention in cancer therapy causing minimal side effects to healthy cells (Sak, 2012).

Curcumin, a polyphenolic compound obtained from the root of the turmeric plant, exhibits antioxidant, anti-inflammatory, and anti-cancer activities in various cancer models including colorectal (Wu et al.,

* Correspondence to: Zeynep Busra Bolat, Molecular Biology and Genetics Department, Hamidiye Institute of Health Sciences, University of Health Sciences, Istanbul 34668, Türkiye.
** Correspondence to: Mehmet H. Ucisik, Department of Genetics and Bioengineering, Faculty of Engineering, Yeditepe University, Kayisdagi Cad, 34755 Istanbul, Atasehir, Türkiye.
E-mail addresses: mehmet.ucisik@yeditepe.edu.tr (M.H. Ucisik), zeynepbusra.bolat@sbu.edu.tr (Z.B. Bolat).

https://doi.org/10.1016/j.tiv.2024.105958
Received 7 February 2024; Received in revised form 10 October 2024; Accepted 20 October 2024
Available online 21 October 2024

2019a), breast (Bimonte et al., 2015), small cell lung (Yang et al., 2012), glioblastoma cancers (Luthra and Lal, 2016) and pancreatic cancer (Hatcher et al., 2008). Curcumin was shown to induce cell apoptosis through the p53 pathway (Fu et al., 2018; Talib et al., 2018). Curcumin acts as a transcription factor when the DNA is damaged, which halts the cell cycle at the G1 phase, creating time for DNA repair. Once the DNA damage becomes irreparable, p53 activates the transcription of the pro-apoptotic gene BAX and the programmed cell death cascade is initiated (Devarajan et al., 2002).

Despite strong anti-cancer activity on pancreas cancer cells (Zhu and Bu, 2017) and low toxicity profile on healthy cells (Chen et al., 2014) curcumin has the limitations of low bioavailability (Kwon and Magnuson, 2007) and solubility (Kurien et al., 2007). The delivery of curcumin within the nanoparticles may provide a means by overcoming these limitations to a more effective and stable therapeutic efficacy (Nasery et al., 2020). Thus, polymeric nanoparticles (Mahmood et al., 2015), solid lipid nanoparticles (Jourghanian et al., 2016) liposomes (Dutta and Bhattacharjee, 2017), silver (Mohammadi et al., 2021) and gold (Amini et al., 2024) nanoformulation were used to deliver curcumin.

Emulsomes are lipoidal vesicular systems composed of an internal solid fat core surrounded by phospholipid (PL) multilayers (Ucisik et al., 2015). Emulsomes with a solid lipid matrix can entrap lipophilic drug compounds in high amounts and provide a prolonged drug release profile (Yilmaz et al., 2020). The characteristics biophysical properties as well as anticancer features of curcumin-loaded emulsomes (CurEm) have been studied in detail previously against various cancer cell models including hepatocellular (Ucisik et al., 2013), prostate (Bolat et al., 2023) and colorectal cancers (Sebaugh, 2011) in vitro. Emulsomes were characterized in these studies as a promising nanocarrier enabling the delivery of low-soluble and unstable curcumin molecules to cancer cells effectively.

Different from these previous studies, the current study investigates the anticancer efficacy of CurEm on the pancreatic cancer PANC-1 cells. The anti-cancer properties of CurEm on PANC-1 cells were assessed thoroughly through cell culture analysis such as cell viability, colony forming assay, scratch assay, and cell cycle arrest. Alterations in P53 pathway and apoptotic-related genes were determined by qPCR analysis. The data obtained provided a novel insight into the molecular mechanisms of CurEm in the inhibition of pancreatic cancer growth and migration and indicated the potential therapeutic value of CurEm in pancreatic cancer therapy.

2. Materials and methods

2.1. Reagents

Curcumin, glyceryl tripalmitate (tripalmitin, purity ≥99 %), 1,2-dipalmitoyl-rac-glycero-3-phosphocholine (DPPC, ~99 %), Cholesterol (≥%99), paraformaldehyde, RNase A and propidium iodide (PI) were purchased from Sigma–Aldrich, Germany. Chloroform (≥ 99.8 %) was obtained from Fluka Chemika, Germany. All chemicals were used as received without further purification. Dimethyl sulfoxide (DMSO) was obtained from Fisher BioReagents, USA. MTS reagent (3-(4,5-di-methylthiazol-2-yl)-5-(3-carboxy-methoxy-phenyl)-2-(4-sulfo-phenyl)-2H-tetrazolium) (CellTiter96 Aqueous One Solution) was supplied by Promega, United Kingdom. Nonidet P-40 was obtained from AppliChem, Germany.

2.2. Production of Emulsome formulations

The CurEm were synthesized and characterized as previously described by Bolat et al., 2023 (Bolat et al., 2023). Briefly, the CurEm was synthesized by using the film hydration method, in which 20 mg tripalmitin, 2 mg dipalmitoyl phosphatidylcholine, and 0.6 mg cholesterol together with curcumin (8 mg) were initially dissolved in the organic solvent, i.e., chloroform (2 mL). The solvent was completely removed in the rotary evaporator. The dry thin film was rehydrated with an aqueous solution (5 mL) and mixed in a rotary evaporator at 80 °C to facilitate emulsome formation. Subsequently, the particles were uniformly homogenized using an ultrasonication bath at a temperature of 70 °C. The unincorporated curcumin in the solution was separated by centrifugation at a speed of 13,200 rpm (16,100 ×g) for 10 min. The supernatant, i.e., CurEm, was taken and kept at 4 °C until further cell culture studies.

2.3. Characterization of emulsome formulations

2.3.1. Size and zeta potential

The mean particle size and zeta potential of emulsomes were determined by dynamic light scattering using a Zetasizer instrument (Nano ZS; Malvern Instruments, UK). Accordingly, samples were diluted in 1 mM KCl solution to suitable concentrations. All analyses were performed in the auto-measuring mode at 25 °C. The average of triplicate analyses was recorded for each sample.

2.3.2. Quantification of curcumin incorporated into CurcuEmulsomes

The concentration of curcumin encapsulated inside CurcuEmulsomes was estimated as described elsewhere (Bolat et al., 2023; Bolat et al., 2020; Yilmaz et al., 2020). A 1 mg/mL stock solution of curcumin was prepared in DMSO. A standard curve, generated by successive dilutions of the stock solution (5, 10, 20, 50, 100 μg/mL) in a 96-well microplate (NEST Scientific, Cat #701001, China), was used to determine curcumin concentrations in samples prepared by 1:10 dilution of CurcuEmulsome suspension in DMSO. Sample absorbance was measured at 430 nm on a UV–vis spectrophotometer (Spectramax i3 Multi-Mode Microplate Reader Detection Platform; Molecular Devices, Sunnyvale, CA, USA). A standard curve was prepared from the values of standards. The curcumin concentration of CurcuEmulsomes was estimated by the readout of the absorbance intensity and corresponding concentration on the standard curve.

2.4. Cell culture

Human pancreatic cancer PANC-1 (CRL-1469) cell lines were purchased from the American Type Culture Collection (ATCC, USA). Cells cultured in DMEM medium (Gibco, Thermo Fisher Scientific, USA) supplemented with 10 % fetal bovine serum (FBS; Gibco, Thermo Fisher Scientific, USA) and 100 units/mL of penicillin, 100 μg/mL of streptomycin and amphotericin (1 % PSA; Gibco, Thermo Fisher Scientific, USA). Cells were maintained in a humidified atmosphere at 37 °C with 5 % CO_2.

2.5. Cell viability assay and morphological changes

The cytotoxicity of CurEm on PANC-1 cells was determined by MTS assay. PANC-1 cells were seeded at a density of 5×10^3 cells/well in 96-well plates. After 24 h (h) of incubation, cells were treated with curcumin or CurEm (0–40 μM). At each 24 h interval, cells were treated with MTS solution according to the manufacturer's instructions and incubated for 2 h. Cell viability was measured by a microplate reader (Biotech ELx800, USA) at 490 nm. Cell viability was determined as percentages by setting the absorbance of the non-treated control (Ctrl) group to 100 %. IC_{50} values were determined using IC_{50} Calculator AAT Bioquest (Pitucha et al., 2020; Sebaugh, 2011).

For observing morphological changes, PANC-1 cells were seeded on 24 well plates with a density of 25,000 cells/well and treated with 30 μM curcumin or CurEm the following day. After 48 h, cells were washed with PBS and added fresh media. Cells were visualized with Paula Cell Imager (S/N 484799, Leica).

2.6. Colony forming assay

For colony forming assay, PANC-1 cells were seeded in a 6-well plate with a density of 500 cells/well. After 24 h, each well was treated with 30 μM curcumin or CurEm following an incubation of 14 days (d). Next, colonies were fixed with methanol for 20 min, stained with 0.1 % crystal violet for 5 min, and washed with PBS. Colony numbers and diameters were counted and evaluated as described previously (Qi et al., 2022) under the light microscope (Primovert, Zeiss).

2.7. Scratch assay

PANC-1 cells were seeded on 6 well plates with a density of 200,000 cells/well. After 24 h, when cells had grown to an 80–75 % confluence, a sterile pipette tip was used to scratch. Cells were treated with 30 μM curcumin or CurEm. Cells were incubated for 24 h and images were captured for each well at 0 and 24 h by Paula Cell Imager (S/N 484799, Leica). The relative distance traveled by the leading edge was assessed and the images were compared and measured by the ratio of scratch closures with the following formula: Scratch Closure rate (%) = [(At = 0 h – At = Δh)/At = 0 h] × 100 (At = 0 h is the area of the scratch measured immediately after scratching. At = Δh is the area of closure measured 24 h after scratching) (Astinfeshan et al., 2019).

2.8. Cell cycle assay

To analyze the cell cycle distribution, PANC-1 (300,000 cells/well) cells were treated with 30 μM curcumin or CurEm and investigated using flow cytometry. After a 48 h incubation period, cells were collected through trypsinization and fixed with 70 % ethanol at 4 °C for at least 1 h. Following fixation, cells were washed twice with cold PBS and stained with a cell cycle solution for 30 min containing a mixture of 10 μg/mL RNase A, 0.01 % non-idet P-40, and 8 μg/mL of PI. Samples were measured using a Guava easyCyte Flow Cytometer (Merck Millipore, Germany) to determine the cell population percentages.

2.9. Quantitative real-time PCR (qRT-PCR)

The total RNA of PANC-1 cells was extracted using TRIzol reagent (VWR Life Science, TriFast) according to the manufacturer's instructions. Complementary DNA (cDNA) was synthesized from total RNA with a cDNA Synthesis kit (Nucleogene). SYBR Green Master Mix (Nepenthe) was applied to perform qPCR (CFX96, BIO-RAD). The Primer sequences were given in Table S1. 18sRNA (Hs_RRN18S_1_SG QuantiTect Primer Assay) housekeeping gene was used for data normalization and $2^{-\Delta\Delta Ct}$ method was used for calculation.

2.10. Western blot analysis

To analyze the protein expression levels, PANC-1 (300,000 cells/well) cells were treated with 30 μM curcumin or CurEm. Cell lysates were isolated using RIPA buffer and the protein concentrations were determined by the BCA Protein Assay. 30 μg of protein was prepared from each protein sample, separated in gel on 12 % SDS-PAGE and transferred to a 0.22 μm PVDF membrane. The membranes were blocked and incubated with un-conjugated Bcl-2, P53 and GAPDH primary antibodies at +4 °C overnight. The membranes were incubated with HRP-conjugated secondary antibodies at 1:5000 dilution for 2 h at room temperature. Finally, interested-specific protein expression levels were detected by the chemiluminescence reagent and analyzed with chemidoc (BIO-RAD).

2.11. Statistical analysis

All data were represented with mean value ± standard deviation (SD). GraphPad Prism (version 8.0.1) software was used to perform statistical analysis and plotting the graphs. Statistical analysis was done using a student *t*-test or two-way ANOVA followed by a post-hoc Tukey test. Differences among treated and non-treated groups were stated as statistically significant at (*) $P \leq 0.05$, (**) $P \leq 0.01$, (***) $P \leq 0.001$, (****) $P \leq 0.0001$.

3. Results

3.1. Physicochemical properties of CurEm

CurEm has been produced and applied for the experimental investigations of at least two separate studies conducted independently. The current study examined the impact of CurEm on the PANC-1 pancreatic cancer cell line, while the other studies investigated the anti-cancer effects of CurEm on LnCAP prostate and HCT116 colon cancer cells, with and without the addition of piperine (Bolat et al., 2023; Bolat et al., 2020; Ucisik et al., 2013). Accordingly, the CurEm had an average diameter of 184.21 ± 13.30 nm with a polydispersity index of 0.19 and a negative zeta potential value of −34.23 ± 4.34 mV, as previously stated.

The average concentration of curcumin in CurEm was estimated to be 0.07 ± 0.02 mg/mL, with an encapsulation efficacy of 4.4 % (Bolat et al., 2023; Ucisik et al., 2013), in which curcumin was used in excess amounts to allow for maximum loading capacity of the lipophilic compound.

3.2. CurEm inhibits cell proliferation and changes the morphology of PANC-1 cells

The optimized CurEm, which is previously described in (Bolat et al., 2020), was used in cell culture studies. The cell viability of 10–40 μM curcumin and CurEm in PANC-1 cells were analyzed by MTS assay for 24 h, 48 h, and 72 h (Fig. 1). Cell viability of curcumin-treated PANC-1

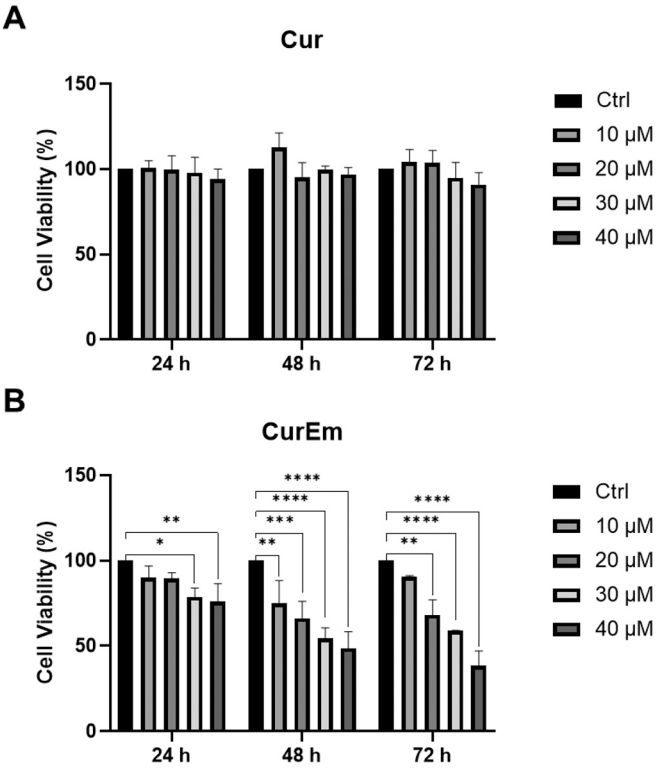

Fig. 1. Cell viability analysis of PANC-1 cells treated with various concentrations (10–40 μM) of **A.** Curcumin (Cur) and **B.** CurEm at 24, 48, and 72 h. Ctrl stands for control group results. Data represents mean ($n = 3$) ± SD (*$P \leq 0.05$, **$P \leq 0.01$, ***$P \leq 0.001$, ****$P \leq 0.0001$).

cells did not vary significantly at all dosage and time points. At 72 h, the highest dose (40 μM) of curcumin showed cell viability of 90.1 % in PANC-1 cells (Fig. 1A). On the contrary, the cell viability of PANC-1 cells treated with CurEm decreased in a time and dose-dependent manner. When PANC-1 cells were treated with 10 and 20 μM CurEm, the cell viability was decreased by 10 % and 11 %, for 24 h, respectively (Fig. 1B). Furthermore, 30 and 40 μM CurEm led to a significant decrease in the cell viability of PANC-1 cells to 22 %, and 24 %, respectively (Fig. 1B). At 48 h, there was a significant decrease of 25 %, 34 %, 46 %, and 51 % cell viability in PANC-1 cells when treated with 10, 20, 30, and 40 μM of CurEm, respectively. At 72 h, significant decreases of 32 %, 41 %, and 62 % were recorded when PANC-1 cells were treated with 20, 30, and 40 μM CurEm, respectively (Fig. 1B). IC_{50} values of CurEm-treated PANC-1 cells were 132.58 μM, 37.76 μM, and 32.43 μM at 24, 48, and 72 h, respectively (Table S2). Furthermore, cell viability of PANC-1 cells when treated with emulsomes showed no significant change in cell viability of PANC-1 cells (Fig. S1) and the IC_{50} value was 156.56 μM for 48 h.

Morphological changes were observed for curcumin and CurEm-treated PANC-1 cells compared with the negative control (Ctrl) group at 48 h. PANC-1 cells started to form a spindle-like morphology when treated with 30 μM Cur, while PANC-1 cells treated with 30 μM CurEm formed a spheroidal morphology. Thus, major morphological alterations and cell detachment of PANC-1 cells were observed CurEm group when compared to the morphology of Ctrl and curcumin group (Fig. S2).

3.3. CurEm decreases Colony formation of PANC-1 cells

The effect of curcumin and CurEm on the proliferation and single-cell to determine the survival ability of the PANC-1 cell line was observed. As shown in Fig. 2, PANC-1 colony numbers and diameters decreased significantly ($P < 0.001$) for the CurEm-treated group in comparison to the control group after 14 d incubation. Images of colonies show less in number for the curcumin and CurEm group when compared to the control group (Fig. 2A). Colony diameters were calculated as 1912 ± 304 μm, 516 ± 122 μm, and 69 ± 3 μm for control, Cur and CurEm group, respectively (Fig. 2B). Colony numbers were 368 ± 183, 118 ± 14, and 5 ± 1.5 for the control, curcumin and CurEm groups, respectively (Fig. 2C). Thus, there was a significant decrease in the colony number and diameter of the CurEm group compared control group.

3.4. CurEm inhibited cell migration in PANC-1 cells

The migration ability of curcumin and CurEm treated PANC-1 cells was calculated between 0 and 24 h by scratch assay. After cells were treated with 30 μM curcumin and CurEm, the scratch gap was measured at 0 h, and the closing distances of the same gaps were measured 24 h later. The closure rates for Ctrl, curcumin, and CurEm treated PANC-1 cells were 72.5 ± 5 %, 35 ± 7.7 %, and 4.25 ± 2.5 %, respectively. Thus, much slower closure was observed for the CurEm group when compared to the control and curcumin group. CurEm was observed to have a greater inhibitory effect on the migration of cancer cells (Fig. 3).

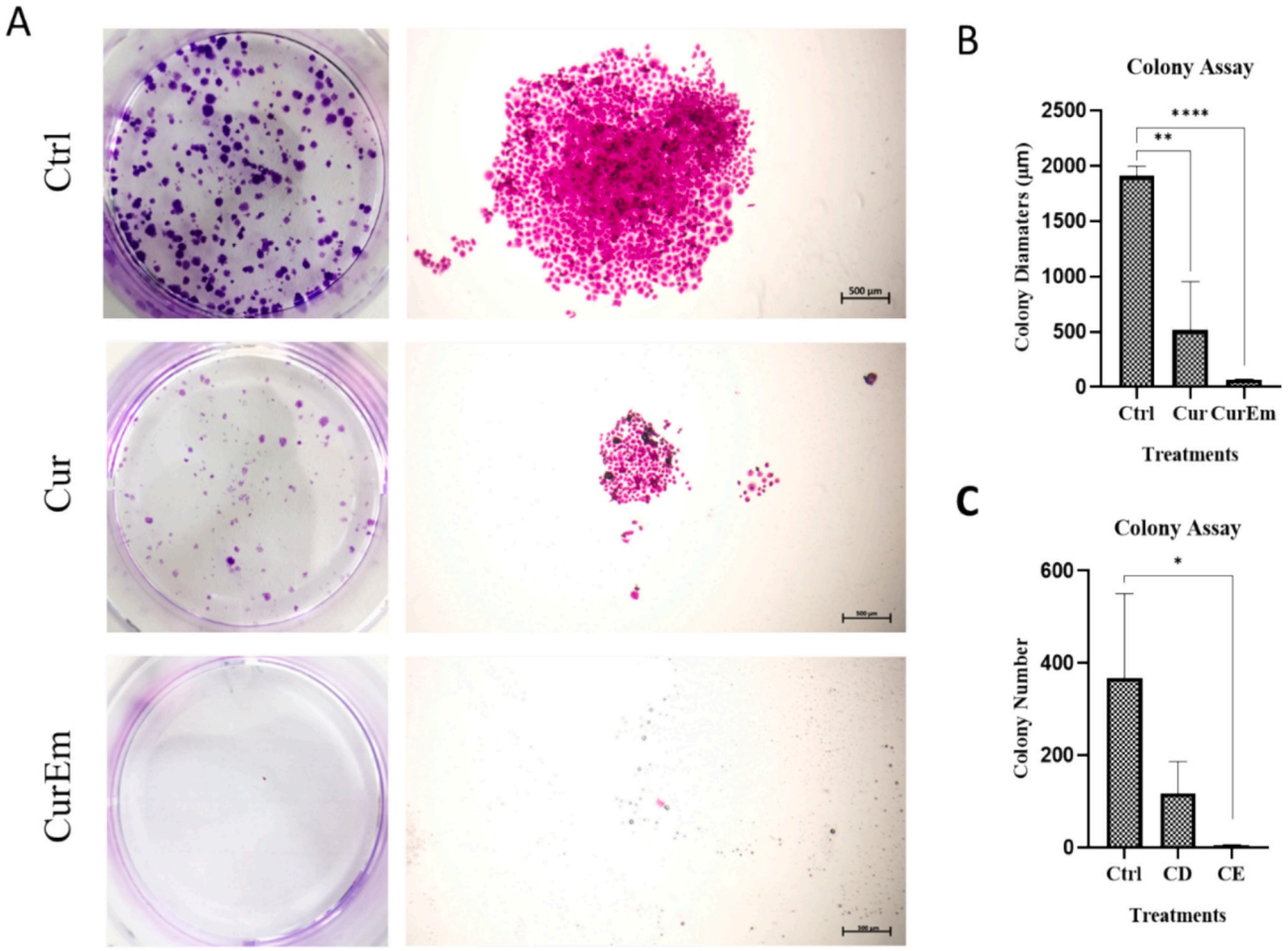

Fig. 2. Colonization of PANC-1 cells upon treatment with 30 μM curcumin (Cur) and 30 μM CurEm for 14d. **A.** Representative of good images of colonies (left panel) and colonies of PANC-1 cells taken with a 10× objective (right panel). Graphical representation of **B.** Colony diameters and **C.** colony numbers for control, curcumin and CurEm treated PANC-1 cells. Data represents mean ($n = 3$) ± SD (*$P \leq 0.05$, **$P \leq 0.01$, ***$P \leq 0.001$, ****$P \leq 0.0001$). Scale bar: 500 μm.

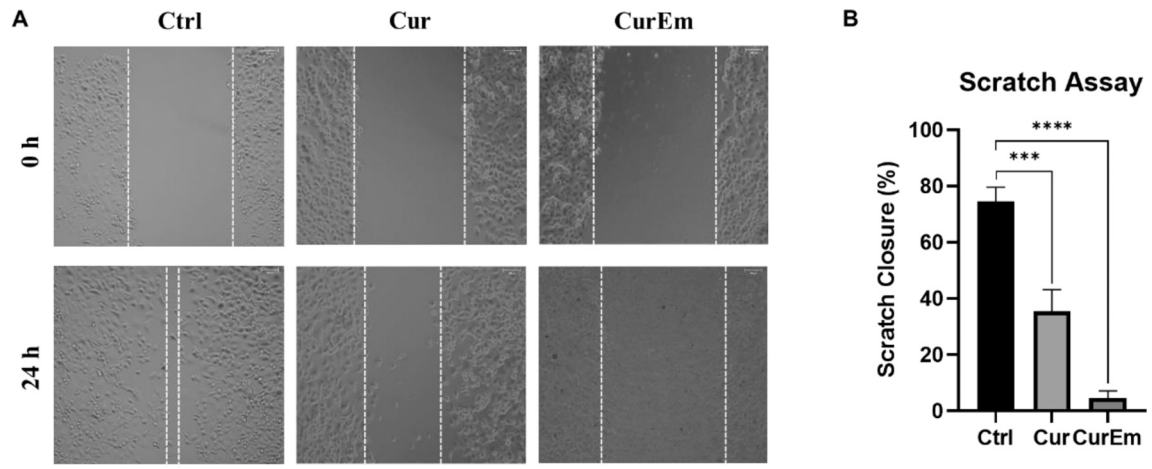

Fig. 3. PANC-1 cells were scratched followed by curcumin (Cur) and CurEm treatment for 24 h. **A.** Images of Ctrl, Cur, and CurEm applications at 0 and 24 h (Scale bar: 100 μm). **B.** Comparison of Cur and CurEm application with Ctrl after 24 h. The graphical representation of the closure rate for control, Cur, and CurEm groups. (***P ≤ 0.001, ****P ≤ 0.0001). n = 3 independent experiments were carried out.

3.5. CurEm induces G2/M arrest in PANC-1 cells

To investigate the cell cycle progression in PANC-1 cells after CurEm treatment, cell cycle distribution after PI staining was analyzed using flow cytometry. The PANC-1 cell population in the G0/G1 phase decreased from 58.27 ± 2.09 % in control cells to 42.06 ± 6.79 % and 46.08 ± 5.79 % in curcumin and CurEm treated PANC-1 cells, respectively. CurEm led to an increase in S phase cell populations, from 18.64 ± 0.27 % in the control group to 21.46 ± 3.87 %. Similarly, curcumin treatment resulted in an increase in S phase cell populations from 18.64 ± 0.27 % to 20.17 ± 4.69 % when compared to untreated cells. The proportion of cell population in the G2/M phase was found to vary depending on the treatment, indicating a cell cycle arrest induced in the G2/M phase after 48 h (Fig. 4). The frequency of the G2/M cell cycle phase increased from 22.99 ± 2.2 % in control cells to 37.77 ± 7.21 % and 32.45 ± 8.68 % for curcumin and CurEm groups, respectively. Thus, these findings revealed that CurEm induces G2/M-phase cell cycle arrest.

3.6. CurEm effect expression levels of apoptotic-related genes in PANC-1 cells

Apoptotic-related gene expression levels of PANC-1 cells were analyzed by qRT-PCR. Our results showed that PANC-1 cells treated with curcumin and CurEm displayed 1.49- and 1.89-fold significant increases in p53 expression compared to control, respectively (Fig. 5A). The treatment of PANC-1 cells with curcumin and CurEm showed a 1.33- and 1.62-fold increase compared to the control for p21 expression levels, respectively (Fig. 5B). CurEm-treated PANC-1 cells expressed significantly higher levels of Caspase 3 by 3.6-fold, compared to untreated cells (Fig. 5C). The expression levels of Bax increased by 1.39 and 2.35-fold for curcumin and CurEm-treated PANC-1 cells, respectively (Fig. 5D). A significant reduction in Bcl-2 expression levels to 0.52-fold was found in CurEm-treated PANC-1 cells (Fig. 5E). Therefore, the CurEm-treated groups exhibited significant alterations in the expression levels of the p53, Caspase3 and Bcl-2 genes.

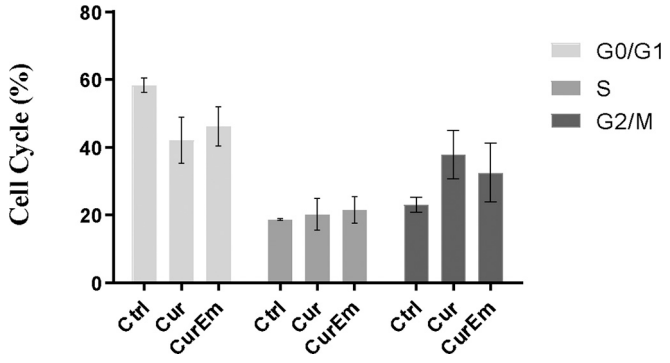

Fig. 4. Cell cycle progression in PANC-1 cells upon treatment with CurEm. Flow cytometry was performed after 30 μM curcumin (Cur) and 30 μM CurEm treatment in PANC-1 cells for 48 h. Error bars represent mean ± SD.

3.7. CurEm effect expression levels of apoptotic-related proteins in PANC-1 cells

It was observed that Bcl-2 expression decreased in Cur-treated PANC-1 cells compared to control. After CurEm treatment, it was observed that Bcl-2 protein expression decreased much more than both the control and Cur-treated PANC-1 cells (Fig. 6A). The Bcl-2 protein expression levels were measured in the bar graph included with the western blot data. When compared to the untreated control cells, there was a significant ($P < 0.05$) reduction in Bcl-2 expression in PANC-1 cells treated with CurEm (Fig. 6B). While an increase in p53 expression was observed in Cur-treated PANC1 cells, p53 expression was interestingly decreased after CuEm treatment (Fig. 6C). Compared to control PANC1 cells, the decrease in p53 expression after CurEm treatment was measured to be statistically significant, $P < 0.0005$ (Fig. 6D).

4. Discussion

Pancreatic cancer stands as one of the most lethal tumors, due to its aggressive behavior and late onset (Du and Shim, 2016; Gillen et al., 2010; McGuigan et al., 2018). While various treatment methods are available for pancreatic cancer, they have not proven to be effective solutions, and thus new treatment approaches are needed. Plants with polyphenolic properties are frequently used in cancer treatment due to their anticancer properties. Curcumin is a natural polyphenol anticancer agent, holding substantial potential in cancer therapy. However, its low water solubility and weak chemical stability limit absorption and bioavailability (Kaminaga et al., 2003; Kunnumakkara et al., 2008). These challenges have prompted the development of novel approaches to deliver curcumin. Emulsomes are biocompatible carriers with a solid lipid core, providing an effective system for substances with low water solubility, such as curcumin. Additionally, their solid cores enable sustained release over an extended period (Heiati et al., 1996; Ucisik et al., 2013; Vyas et al., 2010). Furthermore, Emulsomes does not show

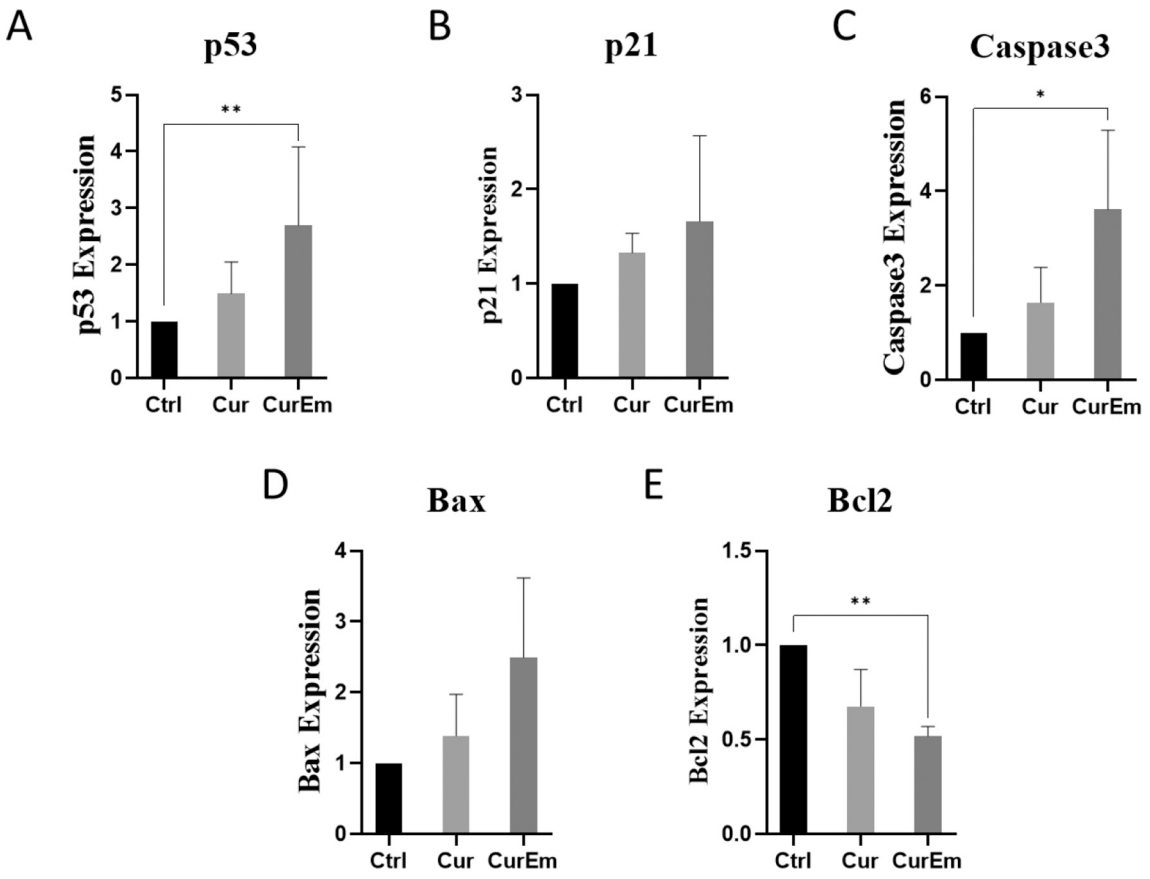

Fig. 5. Relative apoptotic-related gene expression level in PANC-1 cells determined by qRT-PCR. Graph bars for **A.** p53, **B**. p21, **C.** Bax, **D.** caspase3 and **E.** Bcl-2 gene expressions of PANC-1 cells upon treatment with curcumin and CurEm for 48 h. Data represents ($n = 3$) independent experiments ($^{*}P < 0.05$, $^{**}P \leq 0.01$).

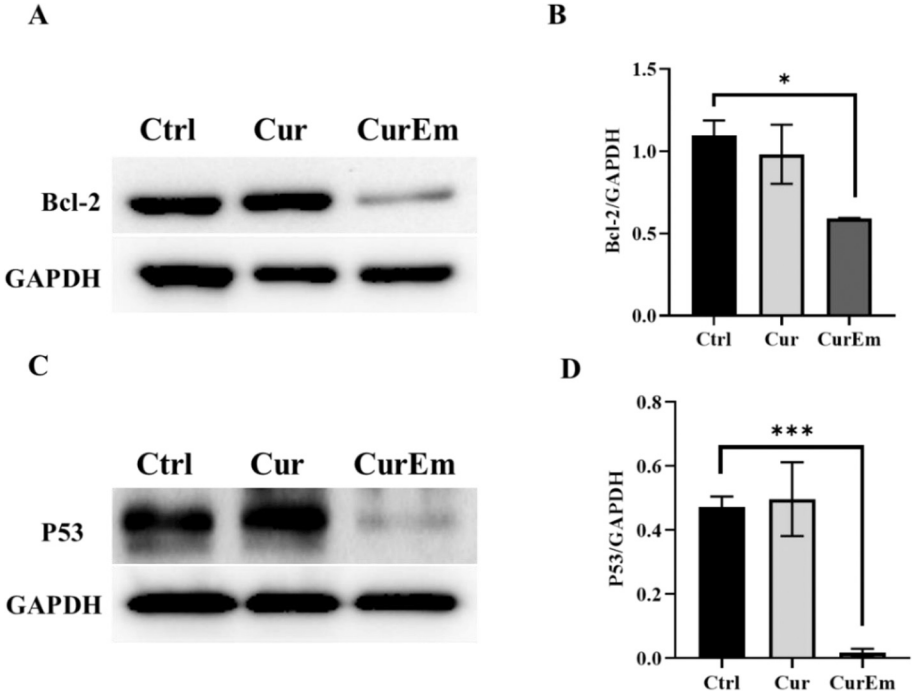

Fig. 6. The results of the western blot analysis show the expression of Bcl-2 and P53 proteins in untreated (Ctrl) PANC1 cells and those treated with Cur or CurEm (A and C). The levels of Bcl-2 and P53 protein expression were measured and presented in a bar graph with the western blot results (B and D). GAPDH was used as the loading control. Data represents (n = 3) independent experiments ($^{*}P < 0.05$, $^{***}P \leq 0.001$).

cytotoxicity in healthy cell lines such as prostate PNT1A cell lines (Bolat et al., 2023). CurEm has been shown as an effective anticancer drug delivery system in HepG2 (Ucisik et al., 2013), LNCaP (Bolat et al., 2023) and HCT116 (Bolat et al., 2020) cell lines. In this study, the molecular mechanisms for the anti-cancer effect of CurEm were investigated on the pancreatic cancer PANC-1 cell line.

The physicochemical characterization studies indicate that the emulsion effectively encapsulates curcumin within its solid inner matrix. CurEm displays a spherical shape and has a smooth phospholipid outer surface, resulting in a stable dispersion. The average diameters were determined using DLS analysis, where the average diameter of CurEm was found to be 184.21 ± 13.30 nm, which is compatible with the literature for drug delivery approaches (Bolat et al., 2023; Bolat et al., 2020; Lee et al., 2010; Oh et al., 2011). It has been suggested that particles smaller than 400 nm can cross vascular endothelial tissue and accumulate at the site of the tumor through the enhanced permeability and retention effect (EPR) ((Bolat et al., 2020),(Gullotti and Yeo, 2009) (Steichen et al., 2013)). Zeta potential also affects the cellular absorption and effectiveness of therapy. It was found that CurEm formulation had a negative zeta potential, i.e., −34.23 ± 4.34 mV, which is further attributed to the contribution of the molecular negative charge of curcumin to the formulation. Although cationic particles have higher rates of internalization compared to negative or neutral particles due to the negatively charged nature of the membrane, cationic-charged nanoparticles have been found to exhibit increased toxicity compared to their neutral or negatively charged counterparts (Albanese and Chan, 2011; Bolat et al., 2020; Cai et al., 2011; Zolnik et al., 2010). Considering the risk factors based on its effectiveness, the CurEm formulation was prepared as negatively charged nanocarriers.

The cell viability data shows that Emulsomes did not have a toxic effect on the PANC-1 cell line compared to the negative control (Fig. S1), indicating that emulsomes are safe to be used as nanocarriers. CurEm significantly inhibits the cell proliferation of PANC-1 cells in a dose- and time-dependent manner. PANC-1 cells treated with all doses of CurEm demonstrate a greater antiproliferative effect compared to the same dosage of curcumin (Fig. 1). The IC_{50} value of CurEm-treated PANC-1 cells was 37.76 μM and this low value can be referred to as an improvement in the efficacy of curcumin by encapsulation of the compound in emulsomes. Previously we have shown that CurEm treatment has a greater anticancer effect than free curcumin treatment in the LNCaP cell line because curcumin carried by emulsomes is chemically more stable and more bioavailable (Bolat et al., 2023). Morphological changes in cell lines from epithelial to spheroid and clustering characteristics are signs of apoptosis (Saraste and Pulkki, 2000). In consistency with the literature, our results show that the morphological change in PANC-1 cells after treatment of CurEm was spheroidal (Fig. S2).

Metastasis of cancer to distant tissues is a result of its ability to migrate (Clark and Vignjevic, 2015). The effect of curcumin has been investigated in many pancreatic cell types, including MIAPaCa-2 (Bimonte et al., 2013), BxPC-3 (Li et al., 2019) and PANC-1 (Cao et al., 2016), showing that curcumin inhibits cell migration and proliferation in these cell lines. Significant suppression of cell migration was observed in the PANC-1 cell line after treatment with 30 μM curcumin at 24 h (Sun et al., 2013). After CurEm treatment we observed a significant decrease in the migration abilities of PANC-1 cells compared to cells treated with control and curcumin group. Inhibiting the migration ability of CurEm-treated PANC-1 cells could be due to the increased stability and bioavailability of CurEm. Cancer cells can proliferate very quickly, which is very important for the development of the cell (Su et al., 2017). The colony formation assay demonstrated a significant decrease in the growth of colonies for curcumin and CurEm-treated PANC-1 cells (Fig. 2).

Controlling the cell cycle progression of cancer cells is one of the most effective parameters that prevent the spread of cancer cells (Weir et al., 2007). Studies show that curcumin arrests the cell cycle in the G2/M phase in the BxPC-3 cell line (Sahu et al., 2009). Furthermore, 40 μM Cur treated PANC-1 cells induce the G2/M arrest phase (Zhu and Bu, 2017). Our results were parallel to the literature, where curcumin and CurEm showed arrest in the G2/M phase in cell cycle analysis. Curcumin is released slowly due to its transport by emulsomes in the solid core structure, and thus cells are exposed to cytotoxic doses for a longer period compared to free curcumin. In addition, the slow release of CurEm caused cell cycle arrest at a lower rate than Cur in the G2/M phase, and similar examples are available in the literature where delivering of curcumin via emulsomes (Ucisik et al., 2013). One important checkpoint in the G1/S phase occurs with the accumulation of the p21 protein, which is a CDK inhibitor and a negative regulator of the cell cycle and serves to provide time for cell repair (Abbas and Dutta, 2009; Fridman and Lowe, 2003). Downregulation and low levels of p21 are associated with a poor and malignant prognosis. P21 gene expression also plays a critical role in the cell cycle and a study conducted on curcumin-treated PANC-1 cells shows an increase in p21 genes along with inhibition of the growth of PANC-1 cells (Shoji et al., 2002) and apoptosis (Zhao et al., 2015). Our results regarding p21 expression levels demonstrate an increase in p21 expression levels of CurEm-treated PANC-1 cells compared to the control group.

P53 contributes to the prevention of entry into mitosis and G2 arrest through multiple pathways, including inhibition of the precursors required for cells to enter mitosis and suppression of genes during the cell cycle. Thus, the p53 gene regulates the G2/M transition (Taylor and Stark, 2001) and cell apoptosis (Roszkowska et al., 2020). Also, the p53 pathway plays an active role in the regulation of metastatic properties such as migration and cell proliferation (Muller et al., 2011). Curcumin affects the p53 pathway, making it an important phytochemical in regulating the development and progression of cancer (Fu et al., 2018; Talib et al., 2018). Our results show that CurEm significantly increased the mRNA expression level of p53 genes in PANC-1 cells. This increase was greater than curcumin-treated PANC-1 cells, showing the delivery of curcumin via emulsomes for a longer period compared to free curcumin in PANC-1 cells. When DNA damage becomes irreparable, p53 activates the transcription of the pro-apoptotic gene BAX and this gene plays a direct role in apoptosis by triggering the release of cytochrome *c* from the mitochondria. The cascade begins with the translocation of cytochrome *c* to the cytoplasm, leading to the activation of caspases and initiating the programmed cell death cascade. Caspase-3, an effector caspase, is a crucial member of this cascade (Devarajan et al., 2002). Our results show that CurEm-treated PANC-1 cells had a significant increase in Caspase 3 genes, while a significant decrease in Bcl-2 genes was detected when compared to the untreated group. Also, an increase was detected in BAX gene expression levels (Fig. 5), suggesting that CurEm successfully activated apoptotic-related genes. Bcl-2 protein levels showed parallel results to gene expression levels. Interestingly we have seen high p53 protein levels in PANC1 cells when treated with free curcumin (Fig. 6). The expression of mutant and wild type p53 protein in untreated PANC-1 cells were shown (Mogaki et al., 1993; Wu et al., 2019b). p53 mutation in cancer promotes uncontrolled cell proliferation and progression of tumors (Liu and Bodmer, 2006) and studies show that curcumin prevents cancer progression through p53 inhibition (Han et al., 1999). Treatment of HCT-15 cells with curcumin resulted in marked down-regulation of p53 at the protein levels (Shehzad et al., 2013), similarly we have seen low p53 protein levels in PANC1 cells when treated with CurEm. However, further analysis should be carried out for p53 pathway for the delivery of curcumin via nanoparticles.

In conclusion, despite the challenges posed by pancreatic cancer, research on natural compounds such as curcumin offers promising solutions for the development of innovative and effective treatment strategies. Curcumin exhibits anti-cancer properties and low toxicity to normal cells, but due to its low bioavailability and stability, it is far from being an effective therapeutic agent. CurEm is promising for overcoming these limitations. Our results show that CurEm inhibits the proliferation and growth of colonies in PANC-1 cells. Also, CurEm decreases the migration ability of PANC-1 cells and causes G2/M arrest in the cell

cycle. Changes in p53, p21, caspase 3, Bcl2, and Bax gene expression levels further provide evidence that CurEm induces apoptosis through the p53 pathway in PANC-1 cells. Considering these results, the delivery of curcumin via emulsomes may be a potential therapeutic agent compared to curcumin in the treatment of pancreatic cancer.

Ethics approval

The authors confirm that no ethical approval is required in the study.

Consent for publication

All authors read and approved for publication.

CRediT authorship contribution statement

Zuleyha Demirci: Writing – original draft, Methodology, Investigation, Data curation. **Zeynep Islek:** Writing – review & editing, Methodology, Investigation. **Halime Ilhan Siginc:** Writing – original draft, Methodology, Investigation. **Fikrettin Sahin:** Writing – review & editing, Resources, Funding acquisition. **Mehmet H. Ucisik:** Writing – review & editing, Supervision. **Zeynep Busra Bolat:** Writing – review & editing, Supervision, Funding acquisition, Conceptualization.

Declaration of competing interest

The authors declare that they have no known competing financial interests or personal relationships that could have appeared to influence the work reported in this paper.

Data availability

The datasets used and/or analyzed in the present study are available from the corresponding author upon reasonable request.

Acknowledgements

The authors thank Cansu Umran Tunc for technical support in flow cytometry.

Appendix A. Supplementary data

Supplementary data to this article can be found online at https://doi.org/10.1016/j.tiv.2024.105958.

References

Abbas, T., Dutta, A., 2009. p21 in cancer: intricate networks and multiple activities. Nat. Rev. Cancer 9, 400–414. https://doi.org/10.1038/nrc2657.

Albanese, A., Chan, W.C.W., 2011. Effect of gold nanoparticle aggregation on cell uptake and toxicity. ACS Nano 5, 5478–5489. https://doi.org/10.1021/NN2007496.

Amini, S.M., Emami, T., Rashidi, M., Zrrinnahad, H., 2024. Curcumin-gold nanoformulation: synthesis, characterizations and biomedical application. Food Biosci. 57, 103446. https://doi.org/10.1016/J.FBIO.2023.103446.

Astinfeshan, M., Rasmi, Y., Kheradmand, F., Karimipour, M., Rahbarghazi, R., Aramwit, P., Nasirzadeh, M., Daeihassani, B., Shirpoor, A., Golineghad, Z., Saboory, E., 2019. Curcumin inhibits angiogenesis in endothelial cells using downregulation of the PI3K/Akt signaling pathway. Food Biosci. 29, 86–93. https://doi.org/10.1016/J.FBIO.2019.04.005.

Bimonte, S., Barbieri, A., Palma, G., Luciano, A., Rea, D., Arra, C., 2013. Curcumin inhibits tumor growth and angiogenesis in an orthotopic mouse model of human pancreatic cancer. Biomed. Res. Int. 2013. https://doi.org/10.1155/2013/810423.

Bimonte, S., Barbieri, A., Palma, G., Rea, D., Luciano, A., D'Aiuto, M., Arra, C., Izzo, F., 2015. Dissecting the role of curcumin in tumour growth and angiogenesis in mouse model of human breast cancer. Biomed. Res. Int. 2015. https://doi.org/10.1155/2015/878134.

Bolat, Z.B., Islek, Z., Demir, B.N., Yilmaz, E.N., Sahin, F., Ucisik, M.H., 2020. Curcumin- and Piperine-loaded Emulsomes as combinational treatment approach enhance the anticancer activity of curcumin on HCT116 colorectal Cancer model. Front. Bioeng. Biotechnol. 8, 505672. https://doi.org/10.3389/FBIOE.2020.00050/BIBTEX.

Bolat, Z.B., Islek, Z., Sahin, F., Ucisik, M.H., 2023. Delivery of curcumin within emulsome nanoparticles enhances the anti-cancer activity in androgen-dependent prostate cancer cell. Mol. Biol. Rep. 50, 2531–2543. https://doi.org/10.1007/S11033-022-08208-0/FIGURES/6.

Cai, J., Yue, Y., Rui, D., Zhang, Y., Liu, S., Wu, C., 2011. Effect of chain length on cytotoxicity and endocytosis of cationic polymers. Macromolecules 44, 2050–2057. https://doi.org/10.1021/MA102498G/ASSET/IMAGES/MEDIUM/MA-2010-02498G_0001.GIF.

Cao, L., Xiao, X., Lei, J., Duan, W., Ma, Q., Li, W., 2016. Curcumin inhibits hypoxia-induced epithelial-mesenchymal transition in pancreatic cancer cells via suppression of the hedgehog signaling pathway. Oncol. Rep. 35, 3728–3734. https://doi.org/10.3892/OR.2016.4709.

Chen, Q., Zheng, Y., Jiao, D. Min, Chen, F. Yuan, Hu, H. Zhen, Wu, Y. Quan, Song, J., Yan, J., Wu, L. Jun, Lv, G. Yuan, 2014. Curcumin inhibits lung cancer cell migration and invasion through Rac1-dependent signaling pathway. J. Nutr. Biochem. 25, 177–185. https://doi.org/10.1016/J.JNUTBIO.2013.10.004.

Clark, A.G., Vignjevic, D.M., 2015. Modes of cancer cell invasion and the role of the microenvironment. Curr. Opin. Cell Biol. 36, 13–22. https://doi.org/10.1016/J.CEB.2015.06.004.

Devarajan, E., Sahin, A.A., Chen, J.S., Krishnamurthy, R.R., Aggarwal, N., Brun, A.M., Sapino, A., Zhang, F., Sharma, D., Yang, X.H., Tora, A.D., Mehta, K., 2002. Down-regulation of caspase 3 in breast cancer: a possible mechanism for chemoresistance. Oncogene 21, 8843–8851. https://doi.org/10.1038/sj.onc.1206044.

Du, B., Shim, J.S., 2016. Targeting epithelial-mesenchymal transition (EMT) to overcome drug resistance in cancer. Molecules 21. https://doi.org/10.3390/MOLECULES21070965.

Dutta, S., Bhattacharjee, P., 2017. Nanoliposomal encapsulates of piperine-rich black pepper extract obtained by enzyme-assisted supercritical carbon dioxide extraction. J. Food Eng. 201, 49–56. https://doi.org/10.1016/J.JFOODENG.2017.01.006.

Fridman, J.S., Lowe, S.W., 2003. Control of apoptosis by p53. Oncogene 22, 9030–9040. https://doi.org/10.1038/sj.onc.1207116.

Fu, H., Wang, C., Yang, D., Wei, Z., Xu, J., Hu, Z., Zhang, Y., Wang, W., Yan, R., Cai, Q., 2018. Curcumin regulates proliferation, autophagy, and apoptosis in gastric cancer cells by affecting PI3K and P53 signaling. J. Cell. Physiol. 233, 4634–4642. https://doi.org/10.1002/JCP.26190.

Gillen, S., Schuster, T., Büschenfelde, C.M. Zum, Friess, H., Kleeff, J., 2010. Preoperative/neoadjuvant therapy in pancreatic cancer: a systematic review and meta-analysis of response and resection percentages. PLoS Med. 7. https://doi.org/10.1371/JOURNAL.PMED.1000267.

Gullotti, E., Yeo, Y., 2009. Extracellularly activated nanocarriers: a new paradigm of tumor targeted drug delivery. Mol. Pharm. 6, 1041–1051. https://doi.org/10.1021/MP900090Z.

Han, S.S., Chung, S.T., Robertson, D.A., Ranjan, D., Bondada, S., 1999. Curcumin causes the growth arrest and apoptosis of B cell lymphoma by downregulation of egr-1, c-myc, bcl-XL, NF-kappa B, and p53. Clin. Immunol. 93, 152–161. https://doi.org/10.1006/CLIM.1999.4769.

Hatcher, H., Planalp, R., Cho, J., Torti, F.M., Torti, S.V., 2008. Curcumin: from ancient medicine to current clinical trials. Cell. Mol. Life Sci. 65, 1631. https://doi.org/10.1007/S00018-008-7452-4.

Heiati, H., Phillips, N.C., Tawashi, R., 1996. Evidence for phospholipid bilayer formation in solid lipid nanoparticles formulated with phospholipid and triglyceride. Pharm. Res. 13, 1406–1410. https://doi.org/10.1023/A:1016090420759/METRICS.

Huang, Q., Zhang, Y., Zheng, Y., Yang, H., Yang, Y., Mo, Y., Li, L., Zhang, H., 2022. Molecular mechanism of curcumin and its analogs as multifunctional compounds against pancreatic cancer. Nutr. Cancer 74, 3096–3108. https://doi.org/10.1080/01635581.2022.2071451.

Jourghanian, P., Ghaffari, S., Ardjmand, M., Haghighat, S., Mohammadnejad, M., 2016. Sustained release curcumin loaded solid lipid nanoparticles. Adv. Pharm. Bull. 6, 17–21. https://doi.org/10.15171/APB.2016.04.

Kaminaga, Y., Nagatsu, A., Akiyama, T., Sugimoto, N., Yamazaki, T., Maitani, T., Mizukami, H., 2003. Production of unnatural glucosides of curcumin with drastically enhanced water solubility by cell suspension cultures of *Catharanthus roseus*. FEBS Lett. 555, 311–316. https://doi.org/10.1016/S0014-5793(03)01265-1.

Kunnumakkara, A.B., Anand, P., Aggarwal, B.B., 2008. Curcumin inhibits proliferation, invasion, angiogenesis and metastasis of different cancers through interaction with multiple cell signaling proteins. Cancer Lett. 269, 199–225. https://doi.org/10.1016/J.CANLET.2008.03.009.

Kurien, B.T., Singh, A., Matsumoto, H., Scofield, R.H., 2007. Improving the solubility and pharmacological efficacy of curcumin by heat treatment. Assay Drug Dev. Technol. 5, 567–576. https://doi.org/10.1089/ADT.2007.064.

Kwon, Y., Magnuson, B.A., 2007. Effect of azoxymethane and curcumin on transcriptional levels of cyclooxygenase-1 and -2 during initiation of colon carcinogenesis. Scand. J. Gastroenterol. 42, 72–80. https://doi.org/10.1080/00365520600825216.

Lee, H., Fonge, H., Hoang, B., Reilly, R.M., Allen, C., 2010. The effects of particle size and molecular targeting on the intratumoral and subcellular distribution of polymeric nanoparticles. Mol. Pharm. 7, 1195–1208. https://doi.org/10.1021/MP100038H.

Li, W., Wang, Z., Xiao, X., Han, L., Wu, Z., Ma, Q., Cao, L., 2019. Curcumin attenuates hyperglycemia-driven EGF-induced invasive and migratory abilities of pancreatic cancer via suppression of the ERK and AKT pathways. Oncol. Rep. 41, 650–658. https://doi.org/10.3892/OR.2018.6833.

Liu, Y., Bodmer, W.F., 2006. Analysis of P53 mutations and their expression in 56 colorectal cancer cell lines. Proc. Natl. Acad. Sci. USA 103, 976–981. https://doi.org/10.1073/PNAS.0510146103.

Luthra, P.M., Lal, N., 2016. Prospective of curcumin, a pleiotropic signalling molecule from *Curcuma longa* in the treatment of glioblastoma. Eur. J. Med. Chem. 109, 23–35. https://doi.org/10.1016/J.EJMECH.2015.11.049.

Mahmood, K., Zia, K.M., Zuber, M., Salman, M., Anjum, M.N., 2015. Recent developments in curcumin and curcumin based polymeric materials for biomedical applications: a review. Int. J. Biol. Macromol. 81, 877–890. https://doi.org/10.1016/J.IJBIOMAC.2015.09.026.

McGuigan, A., Kelly, P., Turkington, R.C., Jones, C., Coleman, H.G., McCain, R.S., . Pancreatic Cancer: A Review of Clinical Diagnosis, Epidemiology, Treatment and Outcomes. http://www.wjgnet.com/, 24, pp. 4846–4861. https://doi.org/10.3748/WJG.V24.I43.4846.

Mogaki, M., Hirota, M., Chaney, W.G., Pour, P.M., 1993. Comparison of p53 protein expression and cellular localization in human and hamster pancreatic cancer cell lines. Carcinogenesis 14, 2589–2594. https://doi.org/10.1093/CARCIN/14.12.2589.

Mohammadi, E., Amini, Seyed Meysam, Mostafavi, S.H., Amini, Seyed Mohammad, 2021. An overview of antimicrobial efficacy of curcumin-silver nanoparticles. Nanomed. Res. J. 6, 105–111. https://doi.org/10.22034/NMRJ.2021.02.002.

Muller, P.A.J., Vousden, K.H., Norman, J.C., 2011. p53 and its mutants in tumor cell migration and invasion. J. Cell Biol. 192, 209. https://doi.org/10.1083/JCB.201009059.

Nasery, M.M., Abadi, B., Poormoghadam, D., Zarrabi, A., Keyhanvar, P., Khanbabaei, H., Ashrafizadeh, M., Mohammadinejad, R., Tavakol, S., Sethi, G., 2020. Curcumin delivery mediated by bio-based nanoparticles: a review. Molecules 25, 689. https://doi.org/10.3390/MOLECULES25030689.

Oh, E., Delehanty, J.B., Sapsford, K.E., Susumu, K., Goswami, R., Blanco-Canosa, J.B., Dawson, P.E., Granek, J., Shoff, M., Zhang, Q., Goering, P.L., Huston, A., Medintz, I. L., 2011. Cellular uptake and fate of PEGylated gold nanoparticles is dependent on both cell-penetration peptides and particle size. ACS Nano 5, 6434–6448. https://doi.org/10.1021/NN201624C.

Pitucha, M., Korga-plewko, A., Kozyra, P., Iwan, M., Kaczor, A.A., 2020. 2,4-Dichlorophenoxyacetic thiosemicarbazides as a new class of compounds against stomach cancer potentially intercalating with DNA. Biomolecules 10, 70. https://doi.org/10.3390/BIOM10020296.

Qi, Y., Zhang, C., Wu, D., Zhang, Y., Zhao, Y., Li, W., 2022. Indole-3-carbinol stabilizes p53 to induce miR-34a, which targets LDHA to block aerobic glycolysis in liver cancer cells. Pharmaceuticals 15, 1257. https://doi.org/10.3390/PH15101257/S1.

Roszkowska, K.A., Gizinski, S., Sady, M., Gajewski, Z., Olszewski, M.B., 2020. Gain-of-function mutations in p53 in cancer invasiveness and metastasis. Int. J. Mol. Sci. 21. https://doi.org/10.3390/IJMS21041334.

Sahu, R.P., Batra, S., Srivastava, S.K., 2009. Activation of ATM/Chk1 by curcumin causes cell cycle arrest and apoptosis in human pancreatic cancer cells. Br. J. Cancer 100, 1425–1433. https://doi.org/10.1038/sj.bjc.6605039.

Sak, K., 2012. Chemotherapy and dietary phytochemical agents. Chemother. Res. Pract. 2012, 1–11. https://doi.org/10.1155/2012/282570.

Saraste, A., Pulkki, K., 2000. Morphologic and biochemical hallmarks of apoptosis. Cardiovasc. Res. 45, 528–537. https://doi.org/10.1016/S0008-6363(99)00384-3/2/45-3-528-FIG2.GIF.

Sebaugh, J.L., 2011. Guidelines for accurate EC50/IC50 estimation. Pharm. Stat. 10, 128–134. https://doi.org/10.1002/PST.426.

Shehzad, A., Lee, J., Huh, T.L., Lee, Y.S., 2013. Curcumin induces apoptosis in human colorectal carcinoma (HCT-15) cells by regulating expression of Prp4 and p53. Mol. Cell 35, 526–532. https://doi.org/10.1007/S10059-013-0038-5.

Shoji, T., Tanaka, F., Takata, T., Yanagihara, K., Otake, Y., Hanaoka, N., Miyahara, R., Nakagawa, T., Kawano, Y., Ishikawa, S., Katakura, H., Wada, H., 2002. Clinical significance of p21 expression in non-small-cell lung cancer. J. Clin. Oncol. 20, 3865–3871. https://doi.org/10.1200/JCO.2002.09.147.

Steichen, S.D., Caldorera-Moore, M., Peppas, N.A., 2013. A review of current nanoparticle and targeting moieties for the delivery of cancer therapeutics. Eur. J. Pharm. Sci. 48, 416–427. https://doi.org/10.1016/J.EJPS.2012.12.006.

Su, J., Zhou, X., Yin, X., Wang, L., Zhao, Z., Hou, Y., Zheng, N., Xia, J., Wang, Z., 2017. The effects of curcumin on proliferation, apoptosis, invasion, and NEDD4 expression in pancreatic cancer. Biochem. Pharmacol. 140, 28–40. https://doi.org/10.1016/J.BCP.2017.05.014.

Sun, X.D., Liu, X.E., Huang, D.S., 2013. Curcumin reverses the epithelial-mesenchymal transition of pancreatic cancer cells by inhibiting the hedgehog signaling pathway. Oncol. Rep. 29, 2401–2407. https://doi.org/10.3892/OR.2013.2385.

Sung, H., Ferlay, J., Siegel, R.L., Laversanne, M., Soerjomataram, I., Jemal, A., Bray, F., 2021. Global cancer statistics 2020: GLOBOCAN estimates of incidence and mortality worldwide for 36 cancers in 185 countries. CA Cancer J. Clin. 71, 209–249. https://doi.org/10.3322/CAAC.21660.

Talib, W.H., Al-Hadid, S.A., Ali, M.B.W., Al-Yasari, I.H., Ali, M.R.A., 2018. Role of curcumin in regulating p53 in breast cancer: an overview of the mechanism of action. Breast Cancer Targets Ther. 10, 207–217. https://doi.org/10.2147/BCTT.S167812.

Taylor, W.R., Stark, G.R., 2001. Regulation of the G2/M transition by p53. Oncogene 20, 1803–1815. https://doi.org/10.1038/sj.onc.1204252.

Ucisik, M.H., Küpcü, S., Schuster, B., Sleytr, U.B., 2013. Characterization of CurcuEmulsomes: nanoformulation for enhanced solubility and delivery of curcumin. J. Nanobiotechnol. 11, 1–13. https://doi.org/10.1186/1477-3155-11-37/FIGURES/10.

Ucisik, M.H., Sleytr, U.B., Schuster, B., 2015. Emulsomes meet S-layer proteins: an emerging targeted drug delivery system. Curr. Pharm. Biotechnol. 16, 392. https://doi.org/10.2174/1389201016041502181126 56.

Vyas, S.P., Subhedar, R., Jain, S., 2010. Development and characterization of emulsomes for sustained and targeted delivery of an antiviral agent to liver. J. Pharm. Pharmacol. 58, 321–326. https://doi.org/10.1211/JPP.58.3.0005.

Weir, N.M., Selvendiran, K., Kutala, V.K., Tong, L., Vishwanath, S., Rajaram, M., Tridandapani, S., Anant, S., Kuppusamy, P., 2007. Curcumin induces G2/M arrest and apoptosis in cisplatin-resistant human ovarian cancer cells by modulating akt and p38 mAPK. Cancer Biol. Ther. 6, 178–184. https://doi.org/10.4161/CBT.6.2.3577.

Wu, C.S., Wu, S.Y., Chen, H.C., Chu, C.A., Tang, H.H., Liu, H.S., Hong, Y.R., Huang, C.Y. F., Huang, G.C., Su, C.L., 2019a. Curcumin functions as a MEK inhibitor to induce a synthetic lethal effect on KRAS mutant colorectal cancer cells receiving targeted drug regorafenib. J. Nutr. Biochem. 74, 108227. https://doi.org/10.1016/J.JNUTBIO.2019.108227.

Wu, S., Xu, Zhi, Chong, H., Wu, X. Lin, Liu, P., Shi, Y. Cong, Pang, P., Deng, L., Zhou, G. Xiong, Chen, X. Yin, 2019b. Dihydrosanguinarine suppresses pancreatic cancer cells via regulation of Mut-p53/WT-p53 and the Ras/Raf/Mek/Erk pathway. Phytomedicine 59. https://doi.org/10.1016/J.PHYMED.2019.152895.

Yang, C.L., Liu, Y.Y., Ma, Y.G., Xue, Y.X., Liu, D.G., Ren, Y., Liu, X.B., Li, Y., Li, Z., 2012. Curcumin blocks small cell lung cancer cells migration, invasion, angiogenesis, cell cycle and neoplasia through Janus kinase-STAT3 signalling pathway. PLoS ONE 7. https://doi.org/10.1371/JOURNAL.PONE.0037960.

Yilmaz, E.N., Bay, S., Ozturk, G., Ucisik, M.H., 2020. Neuroprotective effects of curcumin-loaded emulsomes in a laser axotomy-induced CNS injury model. Int. J. Nanomedicine 15, 9211. https://doi.org/10.2147/IJN.S272931.

Zhao, Z., Li, C., Xi, H., Gao, Y., Xu, D., 2015. Curcumin induces apoptosis in pancreatic cancer cells through the induction of forkhead box O1 and inhibition of the PI3K/Akt pathway. Mol. Med. Rep. 12, 5415–5422. https://doi.org/10.3892/MMR.2015.4060.

Zhu, Y., Bu, S., 2017. Curcumin induces autophagy, apoptosis, and cell cycle arrest in human pancreatic Cancer cells. Evid. Based Complement. Alternat. Med. 2017. https://doi.org/10.1155/2017/5787218.

Zolnik, B.S., González-Fernández, Á., Sadrieh, N., Dobrovolskaia, M.A., 2010. Nanoparticles and the immune system. Endocrinology 151, 458–465. https://doi.org/10.1210/EN.2009-1082.